A Raman Map of the DWCNT RBM Region

R. Pfeiffer*, F. Simon*, H. Kuzmany* and V. N. Popov†

*Institut für Materialphysik, Universität Wien, Vienna, Austria
†Faculty of Physics, University of Sofia, Sofia, Bulgaria

Abstract. Raman studies on double-wall carbon nanotubes (DWCNTs) obtained from peapods showed that the radial breathing mode (RBM) response of the inner tubes is split into more components than there are geometrically possible inner tubes. This was attributed to the possibility that one inner tube type may form in more than one outer tube type. Recent resonance Raman investigations revealed an even more complex and interesting behavior. The split components appear to be grouped into species belonging to the same inner tube chirality and the width of the splitting increases with decreasing tube diameter.

INTRODUCTION

Single-wall carbon nanotubes (SWCNTs) [1] have attracted a lot of scientific interest over the last decade due to their unique structural and electronic properties. By annealing fullerenes enclosed in SWCNTs (so-called peapods [2]) it is possible to transform the fullerenes into a secondary inner tube enclosed in the primary outer tube [3].

A Raman study of the radial breathing modes (RBMs) of the inner tubes revealed that these modes have intrinsic linewidths down to about $0.4\,\mathrm{cm}^{-1}$ [4]. These small linewidths indicate long phonon lifetimes and therefore highly defect free inner tubes, which is a proof for a nano clean-room reactor on the inside of SWCNTs. A closer inspection of the RBM response of the inner tubes revealed that there are more Raman lines than geometrically allowed inner tubes. This was attributed to the possibility that one inner tube type may form in more than one outer tube type [5].

To study this splitting in more detail, we recorded a Raman map of the DWCNT RBM region between 1.54 and 2.54 eV (488 to 803 nm) with a spacing of about 15 meV (where possible). This experiment revealed that the large number of components of the RBMs are strongly grouped into species belonging to the same inner tube chirality. The grouping is retained during the growth process, i.e., members of the groups appear and grow collectively. Additionally, the groups seem to be unaffected of the carbon source filled into the primary tubes (C_{60}, C_{70}, or fullerenes mixed with toluene). Only the outer tubes diameter distribution can influence the intensity distribution within one series. However, the frequencies of the RBM components remain similar over several samples with different outer tubes diameters.

CP786, *Electronic Properties of Novel Nanostructures,* edited by H. Kuzmany, J. Fink, M. Mehring, and S. Roth

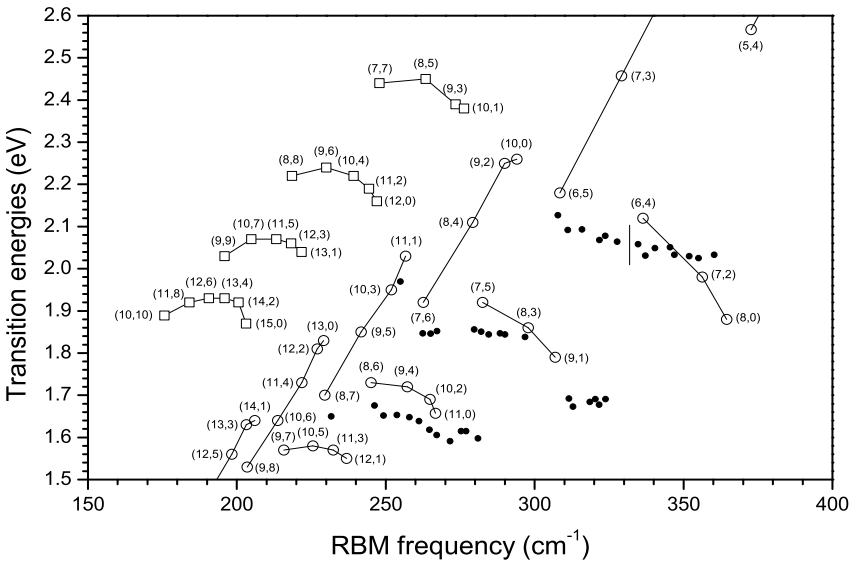

FIGURE 1. Experimental Kataura-plot for dispersed isolated HiPco tubes (open symbols, Refs. [6–9] and for DWCNTs (dots). The number of RBM components of the inner tubes in the DWCNTs was obtained by fitting the normal resolution spectra. Squares and circles denote the E_{11}^{M} and E_{22}^{S} transitions, respectively. Families were completed with calculations after Ref. [10].

EXPERIMENTAL

As starting material for our DWCNTs we used C_{60} peapods which were subsequently annealed at 1250 °C in a dynamic vacuum for 2 hours. The Raman spectra were measured with a Dilor xy triple spectrometer using various lines of an Ar/Kr laser, a dye laser with Rhodamine 6G and Rhodamine 101 as dyes and a Ti:sapphire laser. The spectra were recorded at ambient conditions in normal resolution mode. Selected spectra were recorded in high resolution mode at 90 K.

RESULTS AND DISCUSSION

Figure 1 shows the measured transition energies and RBM frequencies of the inner tubes of DWCNTs and compares it with the published values of dispersed isolated HiPco tubes. One can easily see that the number of RBM components is much larger than the number of geometrically allowed inner tubes. This is especially true for the $(6,5)$ and $(6,4)$ inner tube types. In normal resolution, each of these chiralities has to be assigned more than five components spread over 20 cm^{-1} and more. In high resolution mode, the number of identifiable components increases to more than ten as can be seen from Fig. 2. For the larger diameter inner tubes the width of the splitting is reduced, although

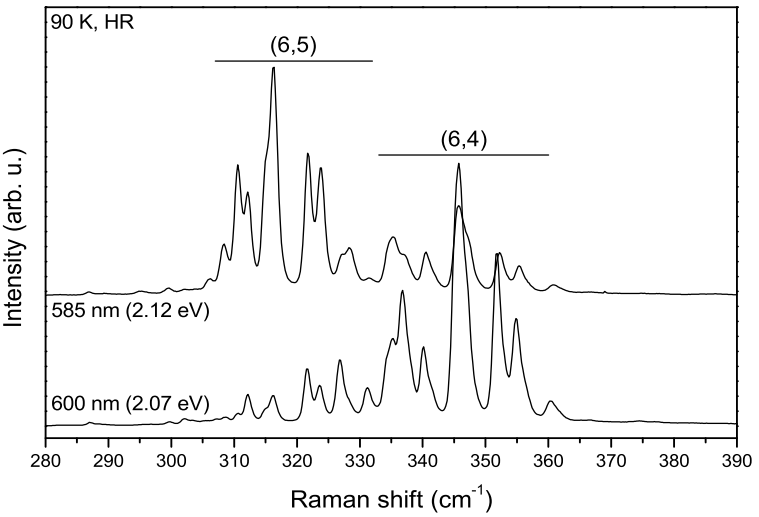

FIGURE 2. RBM response of the $(6,5)$ and $(6,4)$ inner tubes measured in high resolution mode at 90 K. A fit revealed 11 and 14 RBM components for these tubes, respectively.

overlappings of splitting series cannot be ruled out completely. Comparing the RBM frequencies with the HiPco data shows that the lowest frequency components in the groups correspond well to the HiPco frequencies.

The transition energies for all inner tubes are downshifted by about 50 meV as compared to HiPco. Additionally, the transition energies of the components of one inner tube type decrease slightly with increasing RBM frequency.

The transition energies E_{ii} for every inner tube RBM component were obtained by fitting the Stokes resonance Raman profiles with

$$I(E_{\mathrm{L}}) = \frac{A}{\left|(E_{\mathrm{L}} - E_{ii} - i\gamma)(E_{\mathrm{L}} - (E_{ii} + E_{\mathrm{ph}}) - i\gamma)\right|^2}, \tag{1}$$

where E_{L} is the laser excitation energy, E_{ph} is the phonon energy obtained from Raman, and γ is a damping constant. For the example of the 315.9 cm^{-1} RBM component of the $(6,5)$ inner tube (s. Fig. 3), one gets $E_{\mathrm{ph}} = 0.0392\,\mathrm{eV}$, $E_{ii} = 2.0926(6)\,\mathrm{eV}$, and $\gamma = 0.043(1)\,\mathrm{eV}$. If one is only interested in the transition energy, one could also fit a Gaussian to the data points and subtract $E_{\mathrm{ph}}/2$ from the central position (2.1122 eV for the example in Fig. 3). This procedure leads to the same transition energy as above. Usually, the damping constants scattered around 0.05 eV.

The origin of the splitting is still attributed to the interaction of one inner tube type with several outer tubes types of different diameter, but the possible combinations between inner and outer tunes is much larger than anticipated so far. Depending on the outer tube diameter, the inner tube experiences a different hydrostatic pressure which is responsible for the different frequency upshifts as well as for the slight transition energy

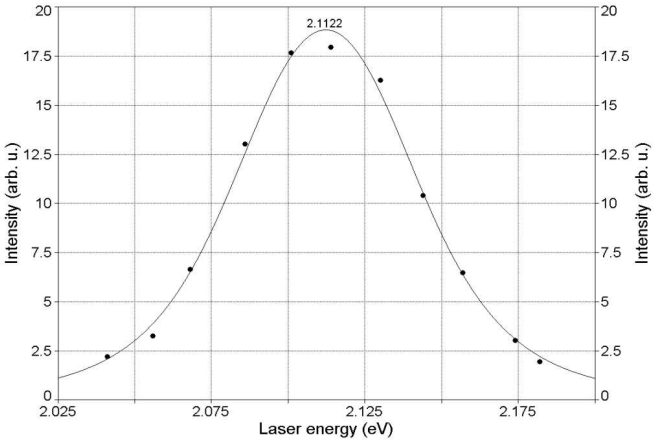

FIGURE 3. Resonance Raman Profile of the $315.9\,\mathrm{cm}^{-1}$ RBM component of the $(6,5)$ inner tube.

red-shifts.

ACKNOWLEDGMENTS

The authors acknowledge financial support from the FWF in Austria, project P17345, and from the EU, project PATONN Marie-Curie MEIF-CT-2003-501099. VNP was supported partly by Marie-Curie MEIF-CT-2003-501080 and partly by NATO CLG 980422. Valuable discussions with Prof. A. Jorio and Prof. A. Rubio are gratefully acknowledged.

REFERENCES

1. Iijima, S., and Ichihashi, T., *Nature*, **363**, 603–605 (1993).
2. Smith, B. W., Monthioux, M., and Luzzi, D. E., *Nature*, **396**, 323–324 (1998).
3. Bandow, S., Takizawa, M., Hirahara, K., Yudasaka, M., and Iijima, S., *Chem. Phys. Lett.*, **337**, 48–54 (2001).
4. Pfeiffer, R., Kuzmany, H., Kramberger, C., Schaman, C., Pichler, T., Kataura, H., Achiba, Y., Kürti, J., and Zólyomi, V., *Phys. Rev. Lett.*, **90**, 225501 (2003).
5. Pfeiffer, R., Kramberger, C., Simon, F., Kuzmany, H., Popov, V. N., and Kataura, H., *Eur. Phys. J. B*, **42**, 345–350 (2004).
6. Bachilo, S. M., Strano, M. S., Kittrell, C., Hauge, R. H., Smalley, R. E., and Weisman, R. B., *Science*, **298**, 2361–2366 (2002).
7. Fantini, C., Jorio, A., Souza, M., Strano, M. S., Dresselhaus, M. S., and Pimenta, M. A., *Phys. Rev. Lett.*, **93**, 147406 (2004).
8. Telg, H., Maultzsch, J., Reich, S., Hennrich, F., and Thomsen, C., *Phys. Rev. Lett.*, **93**, 177401 (2004).
9. Weisman, R. B., and Bachilo, S. M., *Nano Lett.*, **3**, 1235–1238 (2003).
10. Popov, V. N., *New J. Phys.*, **6**, 17 (2004).